

# RSC Advances

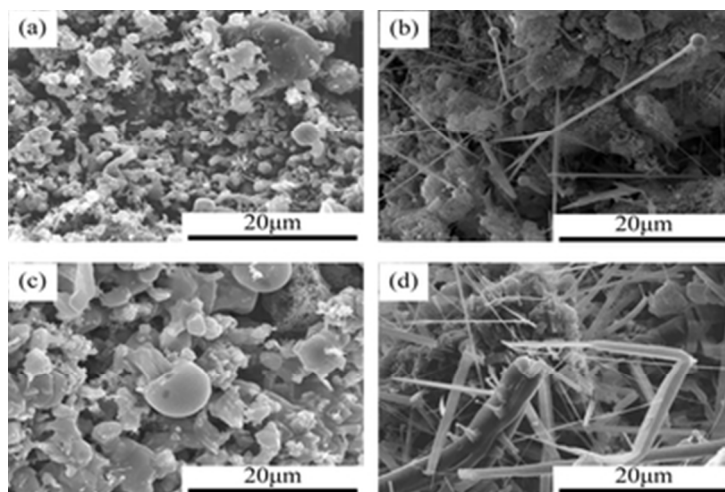


This is an *Accepted Manuscript*, which has been through the Royal Society of Chemistry peer review process and has been accepted for publication.

*Accepted Manuscripts* are published online shortly after acceptance, before technical editing, formatting and proof reading. Using this free service, authors can make their results available to the community, in citable form, before we publish the edited article. This *Accepted Manuscript* will be replaced by the edited, formatted and paginated article as soon as this is available.

You can find more information about *Accepted Manuscripts* in the [Information for Authors](#).

Please note that technical editing may introduce minor changes to the text and/or graphics, which may alter content. The journal's standard [Terms & Conditions](#) and the [Ethical guidelines](#) still apply. In no event shall the Royal Society of Chemistry be held responsible for any errors or omissions in this *Accepted Manuscript* or any consequences arising from the use of any information it contains.



Graphical Abstract  
30x20mm (300 x 300 DPI)

## Synthesis of $\beta$ -Sialon/Ti(C, N) powders from mineral waste residue via carbothermal reduction nitridation

Dexin Yang, Yan-gai Liu\*, Hao Ding, Jian Chen, Zhaohui Huang, Dingyun Ye

*School of Materials Science and Technology, China University of Geosciences  
(Beijing), Beijing 100083, P.R China*

### Abstract

$\beta$ -Sialon/Ti(C, N) composite powders were synthesized via carbothermal reduction nitridation method with low-grade bauxite and ilmenite as starting materials and coke as the reducing agent. The influences of the synthesis temperature, the low-grade bauxite/ilmenite mass ratio, and the amount of coke additive on the phase transformation and morphology of  $\beta$ -Sialon/Ti(C, N) composite powders were investigated with X-ray diffraction, scanning electron microscopy and energy dispersive spectroscopy. The results showed that the optimal experimental conditions for CRN synthesis of  $\beta$ -Sialon/Ti(C, N) composite powders were provided as follows: 4-h treatment, nitrogen atmosphere, and the theoretical coke quantity. When the ratio of ilmenite in raw materials increased from 10% to 50%, the synthesis temperature declined from 1400 °C to 1350 °C. The morphology of well-developed  $\beta$ -Sialon crystals was columnar. After carbothermal reduction nitridation process of ilmenite, the resultant Ti(C, N) particles were distributed dispersedly in the composite powders,

---

\*Corresponding author. Tel.: +86 10 82322186; fax: +86 10 82322186.

E-mail address: liuyang@cugb.edu.cn (Yan-gai Liu).

and either Fe or Fe<sub>3</sub>Si existed in the products depending on the reaction temperature.

*Keywords:* Low-grade bauxite; Ilmenite; Ti(C, N)/β-Sialon powder; CRN

## 1. Introduction

High-grade bauxite is the primary mineral resource of alumina/aluminum industries. However, as the economic reserves of high-grade ores decrease, more researches are focused on the way to process the lower grade ores or bauxite residues at the reasonable cost [1]. Bauxite residues stacked in those residue disposal areas in the world were about 2.7 billion tons, which was increased by about 120 million tons per year [2]. Considerably large amount of low-grade bauxites are stored in the tailing dam after flotation in China and 0.2 ton of aluminosilicate tailing is produced during the processing of one ton bauxite ore according to the flotation method [3]. Thus, how to manage the residues is of growing concern and scientists in worldwide, especially in those countries facing severe environment conditions, are committed to the residue management. In order to solve these issues, the low-grade bauxite or bauxite tailings have been utilized as fillers [3], building materials [4], refractory materials [5], and anticorrosive paints [6].

However, few researchers have used the low-grade bauxite to synthesize the Sialon materials with the carbothermal reduction nitridation (CRN) method, which has been the most promising candidate method for low-cost synthesis of Sialon materials with waste residues and minerals [7-9]. At present, it is commonly known that Sialon materials are solid solutions of Si<sub>3</sub>N<sub>4</sub> in which some of its Si and N atoms are replaced by Al and O, respectively [10]. Their excellent properties of high

toughness, high wear resistance, high strength, good thermal shock resistance, thermostability, and chemical stability offer great potential for many commercial applications [11-12]. Furthermore, wider engineering application of sialon materials could be realized if the sintering temperature could be decreased and the inexpensive raw materials like residues and some minerals could be utilized.

Titanium carbonitride (Ti(C, N)) ceramic powders are widely used to prepare the advanced ceramic-based composite employed in metalworking, electrical and electronics, automotive and refractory industries because of their various excellent properties, such as oxidation resistance, high wear resistance, erosion resistance, high hardness, and high melting point [13-15]. Various methods and starting materials are employed to synthesize Ti(C, N) powders. For instance, Chen *et al.* [16] prepared Ti(C, N) from molten salts via the CRN method. Lugscheider *et al.* [17] produced Ti(C, N) with physical vapor deposition (PVD). Garcia *et al.* [18] made Ti(C, N) with chemical vapor deposition (CVD).

In this paper, we systematically investigated the effects of temperature, the mass ratio of low-grade bauxite to ilmenite, and the carbon content on the preparation of  $\beta$ -Sialon/Ti(C, N) composite powders with the CRN method. The phase transformation, morphology and synthesis mechanism of  $\beta$ -Sialon/Ti(C, N) composite powders were also studied. The purpose of this research was to synthesize  $\beta$ -Sialon and Ti(C, N) composite powders and combine the positive properties of these two kinds of powders, and the as-prepared composite materials would have potential application in metallurgical industry and refractory industry. Besides, the as-prepared

$\beta$ -Sialon/Ti(C, N) powders have successfully used in the unfired  $\text{Al}_2\text{O}_3$ -SiC/ $\beta$ -Sialon/Ti(C, N)-C refractories as one kind of raw materials and Ti(C, N)/ $\beta$ -Sialon powders were able to improve the slag corrosion resistance of the composite refractories [19]. This work would provide the theoretical basis for the production of  $\beta$ -Sialon/Ti(C, N)-based composites, and the feasible technology for the high-efficiency utilization of low-grade bauxite and ilmenite.

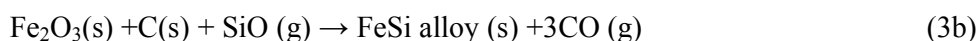
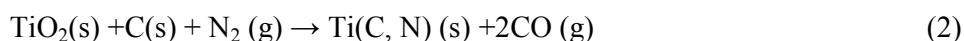
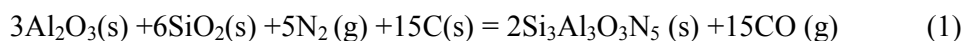
## 2. Materials and methods

### 2.1. Material preparation

The main starting materials employed in this study were as follows: low-grade bauxite (granularity  $\leq 75 \mu\text{m}$ , chemical composition (wt.%):  $\text{Al}_2\text{O}_3$ :48.89,  $\text{SiO}_2$ :44.92,  $\text{TiO}_2$ : 3.64,  $\text{Fe}_2\text{O}_3$ :1.27, others: 1.28, Shanxi Province, China), ilmenite (granularity  $\leq 75 \mu\text{m}$ , chemical composition (wt.%):  $\text{TiO}_2$ : 61.27,  $\text{Fe}_2\text{O}_3$ : 31.23,  $\text{MnO}$ : 2.98,  $\text{Al}_2\text{O}_3$ : 1.26,  $\text{SiO}_2$ : 1.50, others: 1.75, Shandong Province, China), carbon coke powder (granularity  $\leq 75 \mu\text{m}$ , carbon content=88 wt.%, Shanxi Xinshidai Imp. & Exp. Co., Ltd., China). The XRD patterns of low-grade bauxite powder and ilmenite powder were shown in Fig. 1 and Fig. 2. From the figures, we could know that the main phases of the low-grade bauxite were kaolinite ( $\text{Al}_2\text{O}_3 \cdot 2\text{SiO}_2 \cdot 2\text{H}_2\text{O}$ ) and diaspore ( $\text{Al}_2\text{O}_3 \cdot \text{H}_2\text{O}$ ) and that those of the ilmenite were ilmenite ( $\text{FeTiO}_3$ ) and rutile ( $\text{TiO}_2$ ).

The recipe design includes three key points. First, the theoretical stoichiometry is defined by the proportion of low-grade bauxite, ilmenite and coke on the basis of complete nitridation of  $\text{Al}_2\text{O}_3$  and  $\text{SiO}_2$  components in low-grade bauxite as well as  $\text{TiO}_2$  in ilmenite. Second, the target products of low-grade bauxite after CRN

processing are  $\beta$ -Sialon ( $z=3$ ,  $\text{Si}_3\text{Al}_3\text{O}_3\text{N}_5$ ), while those of ilmenite are  $\text{Ti}(\text{C},\text{N})$  and Fe (or FeSi alloy), via reaction Eqs. (1) ~ (3), which take place during the reduction nitridation of  $\text{Al}_2\text{O}_3$ ,  $\text{SiO}_2$ ,  $\text{TiO}_2$ , and  $\text{Fe}_2\text{O}_3$ . Third, the theoretical carbon value refers to the content of coke required for the completion of these reaction equations. Furthermore, excessive carbon addition (excessive addition of 10%, 50%, and 100%) is designed provided that the theoretical carbon addition is right sufficient for the equations.



Based on these equations, the proportions of theoretical stoichiometry as well as excessive carbon conditions can be calculated. The starting material powders were mixed according to Table 1. The mixtures were prepared by mixing the starting material powders with the coke additive according to various low-grade bauxite/ilmenite mass ratios and different coke addition. After starting powders were weighed, agate balls were used as the milling media and mixed with the powder mixture at a ball-to-powder weight ratio of 5:1. The starting materials and agate balls were put into the polyurethane jar and milled for 6 h in anhydrous alcohol. After drying at 80 °C for 12 h, the powder mixtures were uniaxially pressed into cylindrical pellets ( $\Phi 20 \text{ mm} \times \sim 10 \text{ mm}$ ) under a pressure of 25 MPa. Finally, these samples were placed on carbon paper and then placed in the center of a high-temperature

atmospheric furnace. The furnace temperature was initially raised to 1000 °C at a heating rate of 10 °C·min<sup>-1</sup> and then heated at a heating rate of 5 °C·min<sup>-1</sup> to the final temperature (1200, 1300, 1350, 1400, 1450, 1500, 1550, and 1600 °C, respectively) which was maintained for 4 h. High purity flowing nitrogen gas (99.99%) was introduced with a pressure of 0.2 MPa. The samples were finally slowly cooled (3 °C·min<sup>-1</sup>) to room temperature.

## 2.2. Characterization

The phases of products were determined with X-ray diffraction (XRD; D8 Advance diffractometer, Bruker, Germany) under the conditions: Cu K $\alpha_1$  radiation ( $\lambda = 1.5406 \text{ \AA}$ ) with a step of 0.02° (2 $\theta$ ) and a scanning rate of 4°·min<sup>-1</sup>. The morphologies and micro-area chemical analysis of the products were examined by scanning electron microscopy (SEM; JEM-6460LV, JEOL, Japan) equipped with an energy dispersive spectroscopy (EDS; INCA X-sight, Oxford Instrument, UK).

## 3. Results and discussion

### 3.1. Effect of carbon addition on phase formation behavior of products

In order to investigate the influence of carbon addition on the phase formation during the CRN process of low-grade bauxite and ilmenite, the series of L1 and L2 with different coke addition were CRNed at 1500 °C with holding hours of 4 h by *in situ* nitridation reaction. The phases in the products as identified in XRD patterns are shown in Fig. 3 and Figure 2. It could be seen from Fig. 3(a) that,  $\beta$ -Sialon, 15R (SiAl<sub>4</sub>O<sub>2</sub>N<sub>4</sub>) and corundum existed in the samples with the theoretical addition of coke (L1-1) or excessive addition of 10% (L1-2). 15R (SiAl<sub>4</sub>O<sub>2</sub>N<sub>4</sub>) phase was formed via

the reaction Eq. (4).

When the coke content is increased to the contents 50% and 100% above theoretical addition (the samples of L1-3 and L1-4), 12H ( $\text{SiAl}_5\text{O}_2\text{N}_5$ ) phase formed via the reaction Eq. (5) was detected to co-exist with the 15R phase. No  $\beta$ -Sialon phase was detected in these samples. It is probably due to the consumption of silica component in the samples during the formation of SiC via Eq. (6). It was indicated that more coke addition was not conducive to the formation of  $\beta$ -Sialon, but the information of Sialon polytypoids of 12H and 15R. In addition, the phases of SiC were also produced because the carbon in the coke reacted with gaseous SiO via Eq. (6) [20]. The more the added coke was, the more the formed SiC phase was, as indicated from its intensity in XRD patterns (Fig. 3 and Figure 2).



The crystal phases in the CRN products of the series of L2 (the weight ratio of low-grade bauxite to ilmenite was 9:1) are shown in Fig. 3 (b). When the addition of coke was the theoretical quantity, the products of the CRN were  $\beta$ -Sialon, 15R, corundum, Ti(C, N) and Fe. In a qualitative point of view, the peak intensities of 15R and SiC were stronger, but those of  $\beta$ -Sialon were weaker in the sample L2-2 than those in the sample L2-1, indicating that less  $\beta$ -Sialon was formed when the amounts of coke were increased. The results were similar with the results in the series of L1.

Furthermore, when the coke addition was 50 *wt. %* above the theoretical quantity, 12H was detected rather than  $\beta$ -Sialon. A certain amount of graphite phase remained in the series of L2 when coke addition (samples L2-3 and L2-4) was 50 *wt. %* or more above the theoretical quantity. Besides, partial iron phase was transformed into  $\text{Fe}_3\text{Si}$ .

As discussed above, the theoretical quantity of coke is preferred in the series of L1 (bauxite:ilmenite=10:0) and L2 (bauxite:ilmenite=9:1) for the formation of  $\beta$ -Sialon when the samples were sintered at 1500 °C for 4 h. The ilmenite was reduced to Fe and Ti (C, N) as designed in the experimental section.

### 3.2. Effect of synthesis temperature on phase behavior of products

Synthesis temperature was a critical factor for the products during the CRN reaction. In order to better understand the effects of synthesis temperature and starting mixture on the phase composition of final products, the samples of the series of L1 – L4 with the theoretical carbon content (samples L1-1 – L4-1) were CRNed at various temperatures (1200, 1300, 1350, 1400, 1450, 1500, 1550 and 1600 °C) for 4 h. XRD patterns of the products of these samples CRNed at different temperatures are shown in Fig. 4 and Figure 3~6.

As it can be seen that corundum phase ( $\alpha\text{-Al}_2\text{O}_3$ ) which originated from the raw materials disappeared at 1600°C in the samples L1-1 and L2-1, and at 1550°C in the sample L3-1 and at 1500°C in the sample L4-1. It suggests that more ilmenite mineral added in the mixture would get corundum involved in the CRN process. In all samples, partial corundum reacted with silica (cristobalite,  $\text{SiO}_2$ ) to form mullite ( $3\text{Al}_2\text{O}_3 \cdot 2\text{SiO}_2$ ) at 1200 °C where silica phase content was less in the samples with

more ilmenite. The silica phase was then nitridized to be silicon oxynitride ( $\text{Si}_2\text{N}_2\text{O}$ ) and disappeared at 1300 °C. It illustrates that the low-grade bauxite mineral started to be nitridized at this temperature. Mullite and  $\text{Si}_2\text{N}_2\text{O}$  were further nitridized at 1350 °C in the sample L1-1 (without ilmenite) to form  $\beta$ -Sialon which was generated at 1300°C in other samples (with ilmenite). As a result, the mullite phase was nitridized completely at 1400 °C in the sample L1-1, at 1350 °C in sample L2-1 (10% ilmenite), and at 1300 °C in other samples (samples L3-1 and L4-1) with more addition of ilmenite (30% and 50%, respectively). The decomposition temperature of  $\beta$ -Sialon varied in the samples. When the 10% ilmenite was added with bauxite (sample L2-1),  $\beta$ -Sialon remained at 1550 °C. With the increasing addition of ilmenite, however, the temperature of the reaction that  $\beta$ -Sialon disappeared gradually declined. For example, when 50% ilmenite was added (sample L4-1),  $\beta$ -Sialon disappeared at 1400 °C. The intermediate X-phase Sialon were formed during the nitridation process as well in the samples L1-1 and L2-1 at 1400 and 1350 °C, respectively.

As shown in Fig. 4 and Table 3~6, the polytypoid phase 15R was generated in all samples, but its formation temperature was slightly different (1400-1450 °C). Besides, the samples with more ilmenite showed the lower formation temperature of 15R. With the rising temperature, the diffraction peaks of  $\beta$ -Sialon became weaker while those of 15R were stronger, indicating that 15R phase was derived from the decomposition of  $\beta$ -Sialon at high temperatures. In addition, SiC in the samples was generated at 1500-1550°C. According to the results, the optimal reaction temperature was 1450 °C for the synthesis of  $\beta$ -Sialon powders from the sample L1-1.

In the samples with ilmenite (L2-1 to L4-1), the phases of Ti (C, N) and Fe were CRNed from ilmenite at 1200 °C in all the samples. In the reduction and nitridation atmosphere at 1550 °C, the corundum phase was partially transformed into AlN and disappeared at 1600 °C, and the iron (Fe) phase reacted with C/CO and the gaseous SiO. The Fe<sub>3</sub>Si phase was produced at 1550 °C. The AlN and Fe<sub>3</sub>Si phases remained in the products of samples synthesized at 1600 °C for 4h. With the decomposition of β-Sialon, another polytypoid Sialon phase, i.e. 21R, was formed at 1600°C in the all samples with 15R in the products. The coexistence of polytypoids is basically reasonable for Sialon polytypoids are in the block-layer structure [21]. The phase assemblages of final products in the samples with ilmenite included AlN, 15R and 21R, which were basically generated from the low-grade bauxite, as well as the phases of Ti (C, N) and Fe<sub>3</sub>Si due to the nitridation of ilmenite mineral.

It could be seen from Figs. 4b-d that the optimal synthesis temperature for β-Sialon/Ti (C, N) composite powders declined from 1400°C to 1350°C when the mass ratio of ilmenite in raw materials increased from 10% (sample L2-1) to 50% (sample L4-1) in the starting mixtures.

### 3.3. Microstructure of products

In order to understand the effects of starting materials and the synthesis temperature, the microstructure evolution of the samples L1-1 with only low-grade bauxite and the samples L4-1 with both low-grade bauxite and ilmenite (a mass ratio of 50:50) after high-temperature synthesis were discussed in detail.

Fig. 5 shows the SEM micrographs of the samples L1-1 (low-grade bauxite with

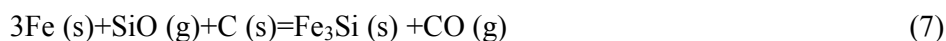
the theoretical quantity of coke) CRNed at 1300 °C, 1350 °C, 1400 °C, 1450 °C, 1500°C, and 1550°C for 4 h. When the reaction temperature was 1300°C (Fig. 5a), the fibrous or columnar  $\beta$ -Sialon was seldom observed, which was consistent with the XRD results that the  $\beta$ -Sialon crystals were not generated at this temperature. When the temperature rose to 1350°C, the fibrous  $\beta$ -Sialon crystals with a spherical droplet could be seen from Fig. 5b. The fibrous crystals are  $\beta$ -Sialon as implied from EDS (Fig. 6) and XRD results (Fig. 4a). Moreover, those spherical droplets on the extremity of the fibres contained Fe, indicating that the  $\beta$ -Sialon fibres were developed via a vapor-liquid-solid (VLS) mechanism [22]. With the temperature rise, the  $\beta$ -Sialon crystals began to grow from fibrous to columnar morphology, and the quantities of  $\beta$ -Sialon crystals also gradually increased in the powders. At 1450 °C, the long columnar crystals could be found and the crystals grew relatively perfectly and reached the maximum amount. These results were consistent with the results of XRD analysis. In addition, it could be proved that the optimal reaction temperature to prepare  $\beta$ -Sialon powders from sample L1-1 was 1450 °C. However, at higher temperatures,  $\beta$ -Sialon crystals began to be decomposed and were not found in the products synthesized at 1500°C or higher temperature. The short laminated polytypoid (15R and 12H) crystals can be observed, as shown in Figs. 5e-f.

SEM micrographs of the samples L4-1 with the theoretical quantity of coke CRNed at 1300°C, 1350 °C, 1400°C, 1450°C, 1500°C and 1550°C for 4 h were shown in Fig. 7. It could be seen that the long columnar crystals, which were the  $\beta$ -Sialon crystals, grew relatively well whose quantity was the largest at 1350 °C than other

reaction temperatures. In addition, Ti (C, N) particles were not well crystallized, and they were distributed dispersedly in the samples L4-1 CRNed at different temperatures (Fig. 7). Besides, the SEM image and the EDS results of sample L4-1 CRNed at 1350 °C for 4 h is shown in Fig. 8. According to the EDS results in Fig. 8b and XRD results in Fig. 4d, the main phase of the detected amorphous sample was Ti (C, N).

In all the products of samples L4-1 CRNed at various temperatures, the spherical particles are shown in Fig. 8. According to the XRD results shown in Fig. 4d, the Fe-related phases are Fe and Fe<sub>3</sub>Si during the phase transformation of the powders. When the temperature was not higher than 1500 °C, Fe phase was generated in the products. At 1550 °C or above, the Fe<sub>2</sub>O<sub>3</sub> component in the starting material ilmenite was nitridized to form Fe<sub>3</sub>Si.

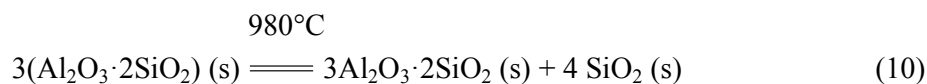
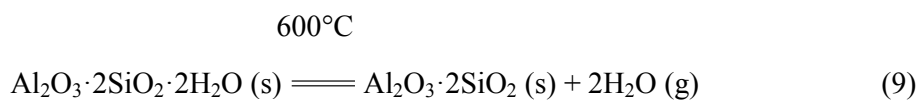
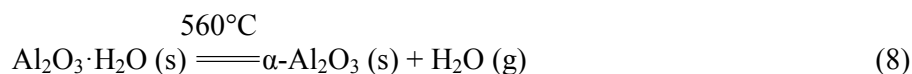
Fig. 9 shows the SEM micrographs and EDS results of the samples sintered at 1450 °C and 1600 °C, respectively. As shown in Fig. 9, both Fe and Fe<sub>3</sub>Si existed in the nitridized products obtained at different reaction temperatures, which was consistent with the results from XRD analysis. Spherical Fe particles were formed at temperatures of 1500 °C or less, and they were conducive to the preferential growth of β-Sialon crystals by VLS mechanism, (Fig. 9a). When the nitrided temperature rose, the faceted Fe<sub>3</sub>Si crystals (Fig. 9b) were produced in the reaction of Fe with gaseous SiO and coke via Eq. (7).



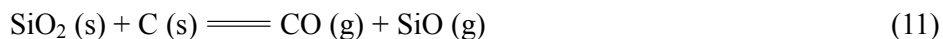
### 3.4. Synthesis mechanism of CRN process of low-grade bauxite and ilmenite.

According to the results above, refractory composites containing  $\beta$ -Sialon and Ti (C, N) could be obtained from low-grade bauxite and ilmenite with the CRN method. The phase transformation in the CRN process of low-grade bauxite could be summarized as follows.

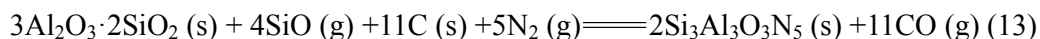
The main phases of the low-grade bauxite included kaolinite ( $\text{Al}_2\text{O}_3 \cdot 2\text{SiO}_2 \cdot 2\text{H}_2\text{O}$ ) and diaspore ( $\text{Al}_2\text{O}_3 \cdot \text{H}_2\text{O}$ ), as shown in Fig. 1. Therefore, in the carbothermal reduction process, dehydration decomposition reaction of low-grade bauxite dominated the early reaction stage, leading to the co-existence of  $\alpha$ - $\text{Al}_2\text{O}_3$ ,  $3\text{Al}_2\text{O}_3 \cdot 2\text{SiO}_2$ , and  $\text{SiO}_2$  (cristobalite) by Eqs. (8-10). In addition, when the reaction temperature rose above  $1100\text{ }^\circ\text{C}$ , the  $\alpha$ - $\text{Al}_2\text{O}_3$  produced from diaspore at  $560\text{ }^\circ\text{C}$  was transformed into corundum.



Then cristobalite ( $\text{SiO}_2$ ) was reduced by C via Eq. (11). Because  $\text{SiO}_2$  was primarily decomposed into silicon monoxide vapor ( $\text{SiO}$ ), the formation of  $\text{Si}_2\text{N}_2\text{O}$  would be dominantly controlled by the diffusion of  $\text{SiO}$  into solid carbon coke structure under nitrogen atmosphere.



When the nitrided temperature rose,  $\text{Si}_2\text{N}_2\text{O}$  was nitrided with  $\text{Al}_2\text{O}_3$  subsequently. Meanwhile, the phases of X-phase, which were the intermediate products of  $\beta$ -Sialon, were generated gradually, and the results were proved by XRD analysis in Fig. 4. Afterwards, the  $\beta$ -Sialon crystals were finally produced during the transformation from the dealumination and nitridation of X-phase. The mullite ( $3\text{Al}_2\text{O}_3 \cdot 2\text{SiO}_2$ ) reacted with gaseous SiO and carbon coke under high-purity nitrogen atmosphere to synthesize the  $\beta$ -Sialon crystals directly via Eq. (13).

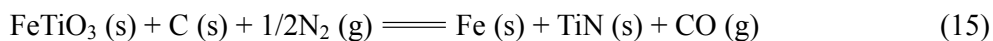


In this experiment, the mass ratio of  $m(\text{SiO}_2)/m(\text{Al}_2\text{O}_3)$  was 0.92 which demonstrated that the element Al was excessive in this recipe. Hence, the corundum co-existed with  $\beta$ -Sialon crystals at 1450 °C, as shown in Fig. 4. In addition, when the nitridation temperature continued to rise, the 15R and 21R were generated from the decomposition of  $\beta$ -Sialon crystals.

The phase transformation in the CRN process of ilmenite was based on the Eqs. (14) and (15).



$$\Delta G_r^\circ = 569818 - 418.35T$$



$$\Delta G_r^\circ = 730000 - 508T$$

According to the overall nitridation reaction of  $\text{Fe}_2\text{O}_3$  and  $\text{TiO}_2$  (Eqs. (14) and (15)), it could be calculated via thermodynamic data that the initial reaction temperatures of Eqs. (14) and (15) are 1362 K (1089 °C) and 1437 K (1164 °C), respectively. Thus, when the temperatures were higher than 1164 °C,  $\text{TiO}_2$  (s) tended to react with C (s) and  $\text{N}_2$  (g) to generate TiC and TiN, respectively. However, both TiC and TiN are of the same crystal structure and their lattice constants are very close. These two phases hardly coexist in the CRN atmosphere. Instead, Ti(C, N) is more expected to be generated, as shown in the XRD results. As a result, Ti (C, N) and Fe/Fe<sub>3</sub>Si was synthesized at above 1200 °C from the CRN of ilmenite.

#### 4. Conclusions

In conclusion, synthesis temperature, low grade bauxite /ilmenite mass ratio, and carbon coke addition affected the carbothermal reduction nitridation (CRN) process of low-grade bauxite and ilmenite. The ideal additive amount of the carbon coke to prepare  $\beta$ -Sialon/Ti (C, N) composite powders was the theoretical quantity. The optimal reaction temperature to synthesize the  $\beta$ -Sialon powders from sample L1-1 (theoretical coke quantity and without ilmenite) was 1450 °C. The optimal CRNed temperature declined from 1400 °C (sample L2-1) to 1350 °C (sample L3-1 and sample L4-1) when the ratio of ilmenite in raw materials increased. In addition, the microstructure of the well-developed  $\beta$ -Sialon crystals was long column and the Ti (C, N) particles were distributed dispersedly in the composite powders. The  $\text{Fe}_2\text{O}_3$

component from the raw material (ilmenite) was CRNed to form Fe at the temperature no higher than 1500 °C and the Fe<sub>3</sub>Si alloy phase was further generated at 1550 °C or higher.

### Acknowledgments

This work was supported by the National Natural Science Foundation of China (Grant No. 51032007), the Fundamental Research Funds for the Central Universities (Grant No. 2012067), the Key Projects in the National Science & Technology Pillar Program (Grant No. 2011BAB03B08) and the Program for New Century Excellent Talents in University of Ministry of Education of China (Grant No. NCET-12-0951).

### References

- [1] P. Smith, *Hydrometallurgy*. 98 (2009) 162-176.
- [2] C. Klauber, M. Gräfe, G. Power, *Hydrometallurgy*. 108 (2011) 11-32.
- [3] Q. H. Lu, Y. H. Hu, *Powder Technol.* 235 (2013) 136-139.
- [4] Huizhi Yang, C. P. Chen, L. J. Pan, H. X. Lu, H. W. Sun, X. Hu, *J. Eur. Ceram. Soc.* 29 (2009) 1887-1894.
- [5] Y. Dong, N. X. Feng, Y. W. Wang, X. L. Wu, *T. Nonferr. Metal. Soc.* 20 (2010) 147-152.
- [6] Q. H. Lu, Y. H. Hu, *T. Nonferr. Metal. Soc.* 22(2012) 483-488.
- [7] V.A. Izhevskiy, L.A. Genova, J.C. Bressiani, F. Aldinger, *J. Eur. Ceram. Soc.* 20 (2000) 2275-2295.
- [8] T. Jiang, X. X. Xue, *T. Nonferr. Metal. Soc.* 22 (2012) 2984-2990.
- [9] F. J. Li, T. Wakihara, J. Tatami, K. Komeya, T. Meguro, *J. Eur. Ceram. Soc.* 27

(2007) 2535-2540.

[10] S. Hampshire, H. K. Park, D. P Thompson and K. H. Jack, *Nature*. 274 (1978) 880-882.

[11] A. R. Bahramian, M. Kokabi, *Appl. Clay. Sci.* 52 (2011) 407-413.

[12] M. Sopicka-Lize, M. Tańcula, T. Wodek, K. Rodak, M. Hüller, V. Kochnev, E. Fokina, K. MacKenzie, *J. Eur. Ceram. Soc.* 28 (2008) 279-288.

[13] D.P. Xiang, Y. Liu, M.J. Tu, et al., *Int. J. Refract. Met. H.* 27 (2009) 111-114.

[14] L. Chen, S.Q. Wang, S.Z. Zhou, et al., *Int. J. Refract. Met. H.* 26 (2008) 456-460.

[15] D. P. Xiang, Y. Liu, et al., *Mater. Charact.* 59 (2008) 241-244.

[16] X. L Chen, Y. B Li, Y. W Li, et al., *Ceram. Int.* 34 (2008) 1253–1259.

[17] E. Lugscheider, O. Knotek et al., *Surf. Coat. Tech.* 116-119 (1999) 239-243.

[18] J. Garcia, R. Pitonak et al., *Surf. Coat. Tech.* 205 (2010) 2322–2327.

[19] De-Xin Yang, Yan-Gai Liun, Ming-Hao Fang, Zhao-Hui Huang, Ding-Yun Ye, *Ceram. Int.* 40 (2014) 1593–1598.

[20] A.W. Weimer, G.A. Eisman, D.W. Susnitzky, D.R. Beaman, J.W. McCoy, *J. Am. Ceram. Soc.* 80 (1997) 2853-2863.

[21] S. F. Huang, Z. H. Huang, Y. G. Liu, M. H. Fang, L. Yin, and J. T. Huang, *J. Am. Ceram. Soc.* 95 (2012) 2044-2050.

[22] S. F. Huang, Z. H. Huang, M. H. Fang, Y. G. Liu, J. T. Huang, and J. Z. Yang, *Cryat. Growth. Des.* 10[6] (2010) 2439-2442.

**Figure captions**

**Fig. 1** XRD patterns of low-grade bauxite raw material.

**Fig. 2** XRD patterns of ilmenite raw material.

**Fig. 3** XRD patterns of samples L1 and L2 with different coke contents CRNed at 1500 °C with holding hours of 4 h.

**Fig. 4** XRD patterns of the samples with different ratios of low-grade bauxite and ilmenite CRNed at different temperatures. (a) sample L1-1, (b) sample L2-1, (c) sample L3-1, (d) sample L4-1 (all with theoretical carbon addition).

**Fig. 5.** SEM micrographs of samples L1-1 with theoretical quantity of coke CRNed at different temperatures for 4 h. (a) 1300°C, (b) 1350°C, (c) 1400°C, (d) 1450°C, (e) 1500°C, (f) 1550°C.

**Fig. 6.** (a) SEM image of sample L1-1 with theoretical quantity of coke CRNed at 1350°C for 4 h; (b) the EDS pattern of area marked by +1 in (a).

**Fig. 7.** SEM micrographs of samples L4-1 with theoretical quantity of coke CRNed at different temperatures for 4 h. (a) 1300°C, (b) 1350°C, (c) 1400°C, (d) 1450°C, (e) 1500°C.

**Fig. 8.** (a) SEM image of sample L4-1 with theoretical quantity of coke CRNed at 1350°C for 4 h; (b) the EDS pattern of area marked by +1 in (a).

**Fig. 9.** SEM micrographs of sample L4-1 with theoretical quantity of coke CRNed at different temperature for 4 h. (a) 1450 °C, (b) 1600 °C, (e) and (f) the EDS patterns of areas marked by +1 and +2 in (a) and (b), respectively.

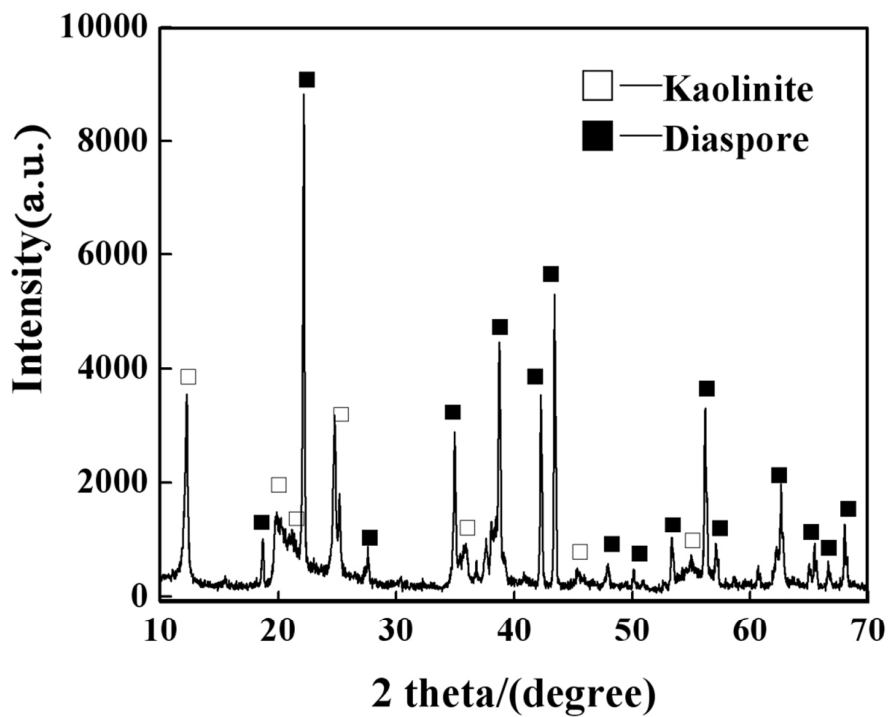


Fig. 1 XRD patterns of low-grade bauxite raw material.

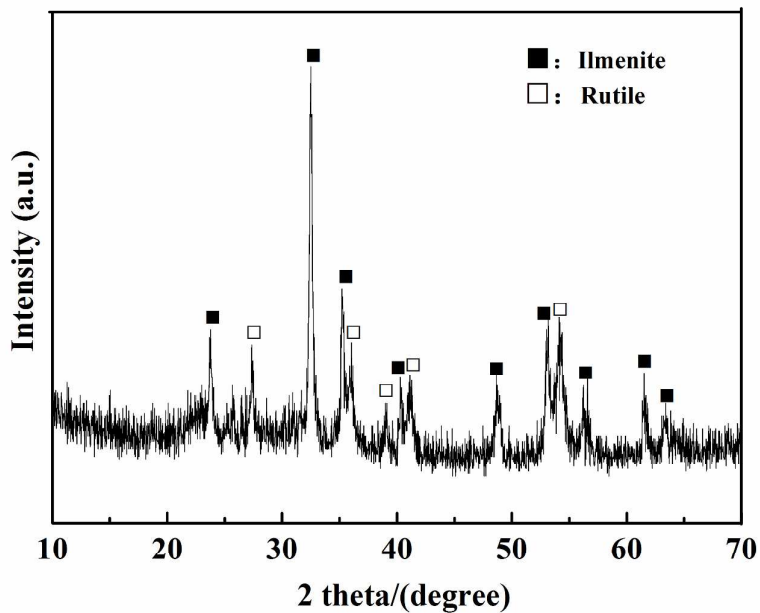
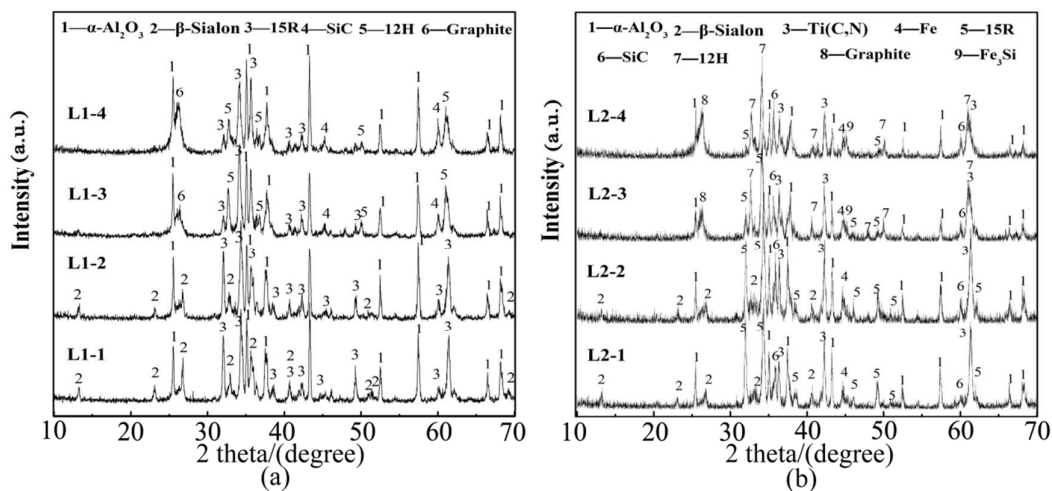
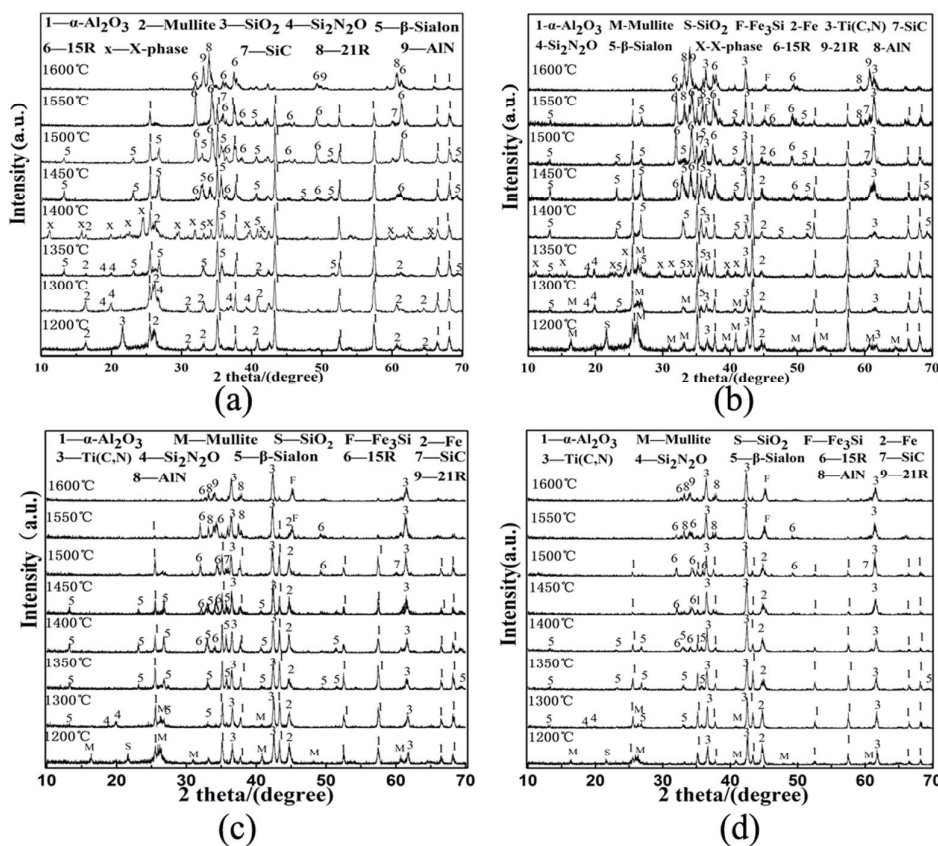


Fig. 2 XRD patterns of ilmenite raw material.



**Fig. 3** XRD patterns of samples L1 and L2 with different coke contents CRNed at

1500 °C with holding hours of 4 h.



**Fig. 4** XRD patterns of the samples with different ratios of low-grade bauxite and

ilmenite CRNed at different temperatures. (a) sample L1-1, (b) sample L2-1, (c)

sample L3-1, (d) sample L4-1 (all with theoretical carbon addition).

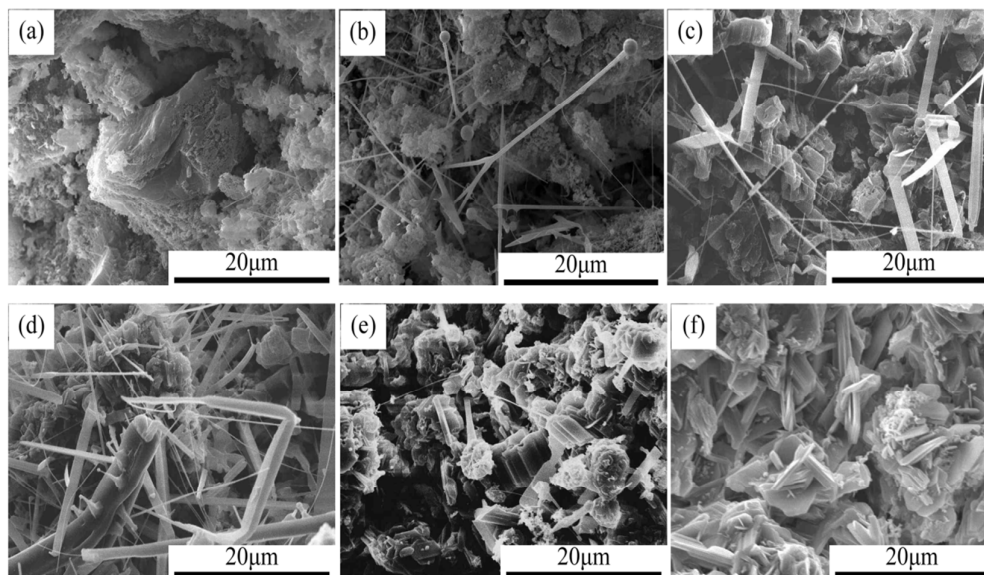


**Fig. 5.** SEM micrographs of samples L1-1 with theoretical quantity of coke CRNed at different temperatures for 4 h. (a) 1300°C, (b) 1350°C, (c) 1400°C, (d) 1450°C, (e) 1500°C, (f) 1550°C.

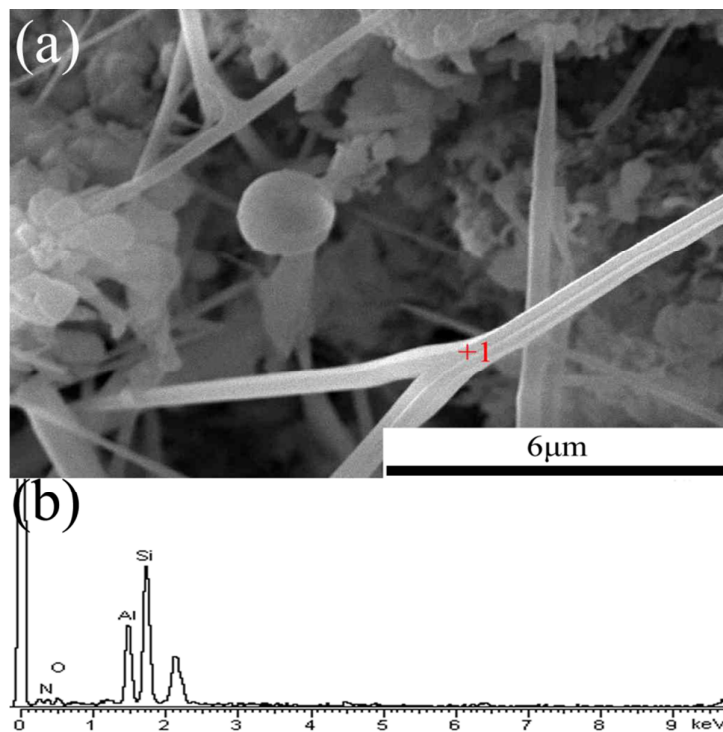


**Fig. 6.** (a) SEM image of sample L1-1 with theoretical quantity of coke CRNed at 1350°C for 4 h; (b) the EDS pattern of area marked by +1 in (a).

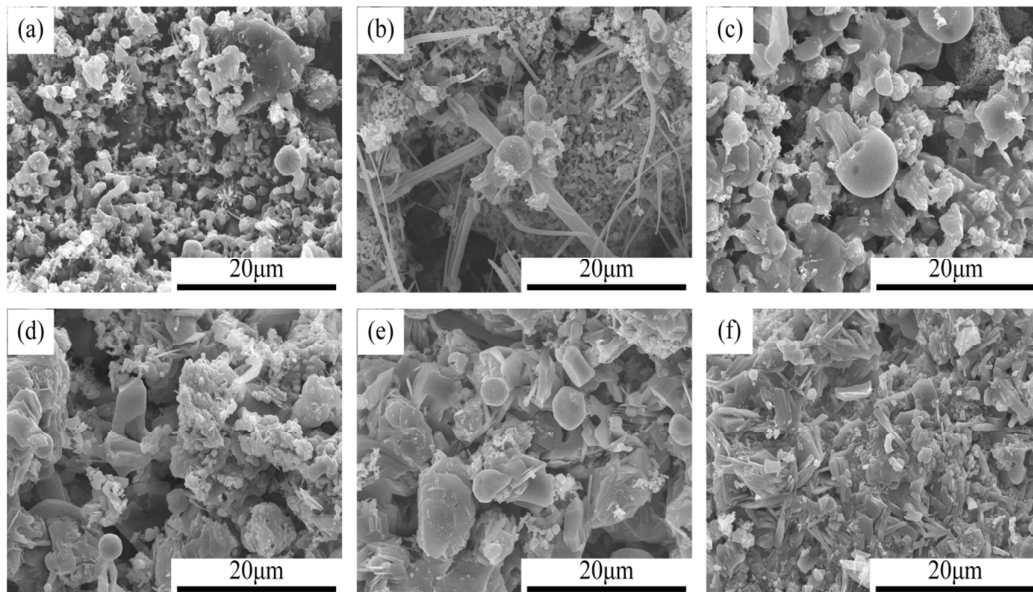


**Fig. 7.** SEM micrographs of samples L4-1 with theoretical quantity of coke CRNed at different temperatures for 4 h. (a) 1300°C, (b) 1350°C, (c) 1400°C, (d) 1450°C, (e) 1500°C.

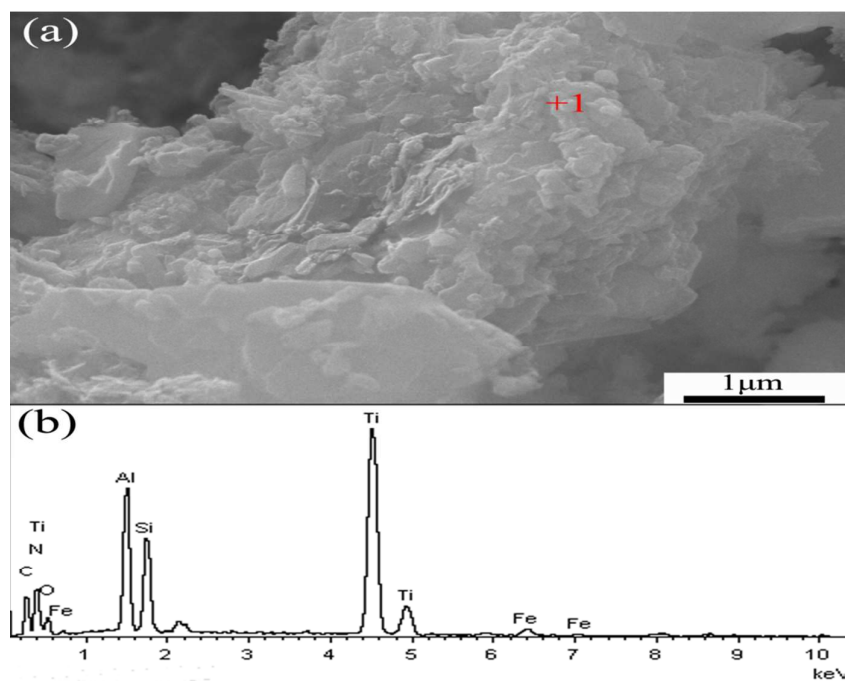


**Fig. 8.** (a) SEM image of sample L4-1 with theoretical quantity of coke CRNed at 1350°C for 4 h; (b) the EDS pattern of area marked by +1 in (a).

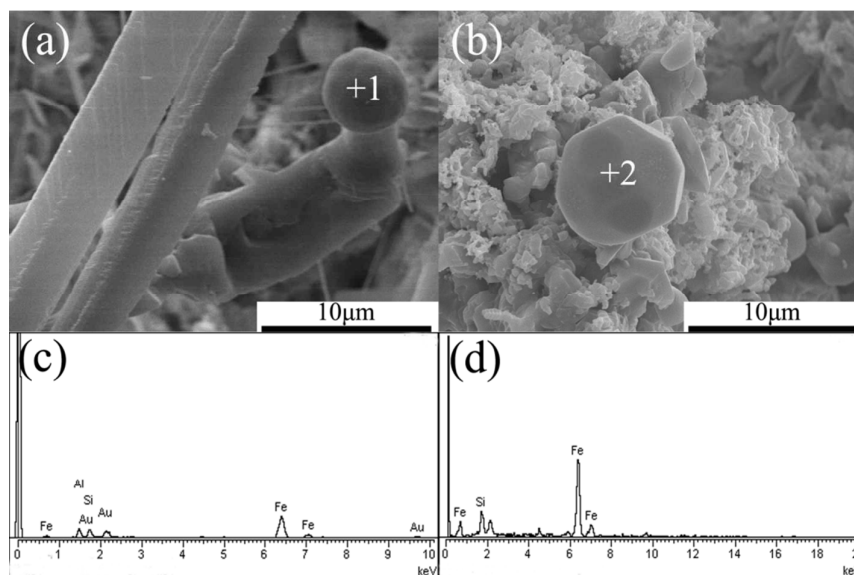


**Fig. 9.** SEM micrographs of sample L4-1 with theoretical quantity of coke CRNed at different temperature for 4 h. (a) 1450 °C, (b) 1600 °C, (e) and (f) the EDS patterns of areas marked by +1 and +2 in (a) and (b), respectively.

## Tables

**Table 1.** Starting compositions of the samples. (wt.%).

**Table 2.** Phase composition of the synthesized powders corresponding to Fig. 3.

**Table 3.** Phase composition of the synthesized powders corresponding to Fig. 4(a).

**Table 4.** Phase composition of the synthesized powders corresponding to Fig. 4(b).

**Table 5.** Phase composition of the synthesized powders corresponding to Fig. 4(c).

**Table 6.** Phase composition of the synthesized powders corresponding to Fig. 4(d).

**Table 1.** Starting compositions of the samples. (wt.%).

Series	Low-grade bauxite	ilmenite	Addition of carbon coke	Samples
L1	100	0	theoretical addition	L1-1
			excess carbon 10%	L1-2
			excess carbon 50%	L1-3
			excess carbon 100%	L1-4
L2	90	10	theoretical addition	L2-1
			excess carbon 10%	L2-2
			excess carbon 50%	L2-3
			excess carbon 100%	L2-4
L3	70	30	theoretical addition	L3-1
			excess carbon 10%	L3-2
			excess carbon 50%	L3-3
			excess carbon 100%	L3-4
L4	50	50	theoretical addition	L4-1
			excess carbon 10%	L4-2
			excess carbon 50%	L4-3
			excess carbon 100%	L4-4

**Table 2. Phase composition of the synthesized powders corresponding to Fig. 3.**

Specimens	Synthesis		Major Phase(s)				Minor Phase(s)
	Temperature/°C						
L1-1	1500	Al <sub>2</sub> O <sub>3</sub>	β-Sialon	15R	—	—	—
L1-2	1500	Al <sub>2</sub> O <sub>3</sub>	β-Sialon	15R	—	—	—
L1-3	1500	Al <sub>2</sub> O <sub>3</sub>	15R	12H	—	—	SiC and Graphite
L1-4	1500	Al <sub>2</sub> O <sub>3</sub>	15R	12H	—	—	SiC and Graphite
L2-1	1500	Al <sub>2</sub> O <sub>3</sub>	β-Sialon	Ti(C, N)	15R	—	Fe and SiC
L2-2	1500	Al <sub>2</sub> O <sub>3</sub>	β-Sialon	Ti(C, N)	15R	—	Fe and SiC
L2-3	1500	Al <sub>2</sub> O <sub>3</sub>	12H	Ti(C, N)	15R	—	Fe, SiC, Graphite and Fe <sub>3</sub> Si
L2-4	1500	Al <sub>2</sub> O <sub>3</sub>	12H	Ti(C, N)	—	15R	15R, Fe, SiC, Graphite and Fe <sub>3</sub> Si

**Table 3. Phase composition of the synthesized powders corresponding to Fig. 4(a).**

Specimens	Synthesis		Major Phase(s)			Minor Phase(s)
	Temperature/°C					
L1-1	1200	Al <sub>2</sub> O <sub>3</sub>	Mullite	—	—	SiO <sub>2</sub>
L1-1	1300	Al <sub>2</sub> O <sub>3</sub>	Mullite	—	—	Si <sub>2</sub> N <sub>2</sub> O
L1-1	1350	Al <sub>2</sub> O <sub>3</sub>	β-Sialon	—	—	Mullite and Si <sub>2</sub> N <sub>2</sub> O
L1-1	1400	Al <sub>2</sub> O <sub>3</sub>	β-Sialon	X-Phase	—	Mullite
L1-1	1450	Al <sub>2</sub> O <sub>3</sub>	β-Sialon	15R	—	—
L1-1	1500	Al <sub>2</sub> O <sub>3</sub>	β-Sialon	15R	—	—
L1-1	1550	Al <sub>2</sub> O <sub>3</sub>	15R	—	—	β-Sialon and SiC
L1-1	1600	15R	21R		—	Al <sub>2</sub> O <sub>3</sub> and AlN

**Table 4. Phase composition of the synthesized powders corresponding to Fig. 4(b).**

Specimens	Synthesis	Major Phase(s)				Minor Phase(s)
	Temperature/°C					
L2-1	1200	Al <sub>2</sub> O <sub>3</sub>	Mullite	—	—	Fe, SiO <sub>2</sub> and Ti(C, N)
L2-1	1300	Al <sub>2</sub> O <sub>3</sub>	Ti(C, N)	Mullite	—	Fe, Si <sub>2</sub> N <sub>2</sub> O and β-Sialon
L2-1	1350	Al <sub>2</sub> O <sub>3</sub>	β-Sialon	X-Phase	Ti(C, N)	Fe, Si <sub>2</sub> N <sub>2</sub> O and Mullite
L2-1	1400	Al <sub>2</sub> O <sub>3</sub>	β-Sialon	Ti(C, N)	—	Fe
L2-1	1450	Al <sub>2</sub> O <sub>3</sub>	β-Sialon	Ti(C, N)	15R	Fe
L2-1	1500	Al <sub>2</sub> O <sub>3</sub>	β-Sialon	Ti(C, N)	15R	Fe and SiC
L2-1	1550	Al <sub>2</sub> O <sub>3</sub>	15R	Ti(C, N)	AlN	Fe <sub>3</sub> Si, β-Sialon, SiC
L2-1	1600	15R	21R	AlN	Ti(C, N)	Fe <sub>3</sub> Si

**Table 5. Phase composition of the synthesized powders corresponding to Fig. 4(c).**

Specimens	Synthesis	Major Phase(s)			Minor Phase(s)
	Temperature/°C				
L3-1	1200	Al <sub>2</sub> O <sub>3</sub>	Mullite	Ti(C, N)	Fe and SiO <sub>2</sub>
L3-1	1300	Al <sub>2</sub> O <sub>3</sub>	Ti(C, N)	—	Fe, Si <sub>2</sub> N <sub>2</sub> O, Mullite and β-Sialon
L3-1	1350	Al <sub>2</sub> O <sub>3</sub>	β-Sialon	Ti(C, N)	Fe
L3-1	1400	Al <sub>2</sub> O <sub>3</sub>	β-Sialon	Ti(C, N)	Fe, 15R
L3-1	1450	Al <sub>2</sub> O <sub>3</sub>	β-Sialon	Ti(C, N) and 15R	Fe
L3-1	1500	Al <sub>2</sub> O <sub>3</sub>	Ti(C, N)	15R	Fe and SiC
L3-1	1550	15R	Ti(C, N)	AlN	Al <sub>2</sub> O <sub>3</sub> , Fe and Fe <sub>3</sub> Si
L3-1	1600	AlN	Ti(C, N)	—	Fe <sub>3</sub> Si, 15R and 21R

**Table 6. Phase composition of the synthesized powders corresponding to Fig. 4 (d).**

Specimens	Synthesis		Major Phase(s)			Minor Phase(s)
	Temperature/°C					
L4-1	1200	Al <sub>2</sub> O <sub>3</sub>	Mullite	Ti(C, N)		Fe and SiO <sub>2</sub>
L4-1	1300	Al <sub>2</sub> O <sub>3</sub>	Ti(C, N)	—		Fe, Si <sub>2</sub> N <sub>2</sub> O, Mullite and β-Sialon
L4-1	1350	Al <sub>2</sub> O <sub>3</sub>	β-Sialon	Ti(C, N)		Fe
L4-1	1400	Al <sub>2</sub> O <sub>3</sub>	Ti(C, N)	—		Fe, 15R and β-Sialon
L4-1	1450	Ti(C, N)	—	—		Fe, Al <sub>2</sub> O <sub>3</sub> and 15R
L4-1	1500	Ti(C, N)	15R	—		Fe, Al <sub>2</sub> O <sub>3</sub> and SiC
L4-1	1550	15R	Ti(C, N)	AlN		Fe <sub>3</sub> Si
L4-1	1600	AlN	Ti(C, N)	—		Fe <sub>3</sub> Si, 15R and 21R